International Journal of Frontiers in Engineering Technology
ISSN 2706-655X Vol.3, Issue 6: 47-52, DOI: 10.25236/IJFET.2021.030605

# Study on reaction mechanism of nitrogen dioxide detection by diazotization coupling reaction

**Zhaoxiang Li[a,*], Xiaogang Mu, Bo Liu, Youzhi Zhang and Xuanjun Wang**

*Xi'an Hi-tech Research Institute, Xi'an, Shaanxi, China*
*[a]984250130@qq.com*
** Corresponding author*

***Abstract:*** *The detection of nitrogen dioxide in air is based on the principle that nitrite diazotization and coupling reaction produce azo compounds. The reaction mechanism is explored by using the method of quantum chemistry. The reaction path is searched by using density functional theory at the level of B3LYP/6-311++G(D,P) The geometric configuration optimization, frequency calculation and thermodynamic function calculation of the transition state and product were carried out, the single point energy and zero correction energy were obtained, the potential energy profile of the reaction was constructed, the activation energy of the reaction was calculated, the TDDFT calculation of the product was carried out, and the UV-vis Spectrum was obtained.*

***Keywords:*** *Nitrogen dioxide, Density functional theory, Quantum chemical calculation*

## 1. Introduction

With the continuous development of industrialization and urbanization, air pollution is becoming more and more serious, and global environmental problems are becoming more and more prominent. Nitrogen dioxide, as a main pollutant in the air, has been widely concerned and studied [1]. Nitrogen dioxide mainly comes from the combustion of fossil fuels. Nitrogen dioxide will also be produced in electric welding, explosive explosion, lightning and microbial action. Nitrogen dioxide will aggravate air pollution, destroy the ozone layer, produce acid rain, photochemical smog[2-3] and PM2.5[4], etc., which not only pollutes the air, but also endangers human health. Nitrogen dioxide is a highly toxic chemical, which will cause a variety of damage to human body after inhalation. Nitrogen dioxide can stimulate respiratory tract and cause ventilation obstruction. If inhaled for a long time, it will significantly reduce human lung capacity and resistance, and damage human nervous system and cardiovascular system [5-6].

In recent years, a variety of detection methods of nitrogen dioxide have been studied at home and abroad. Among them, the conversion of nitrogen dioxide into nitrite ion and the formation of colored azo compounds by the characteristic color reaction of nitrite are the most simple, direct and effective. It is also the recommended method of national standard. Taking p-aminobenzenesulfonic acid and 1-naphthylamine as examples, according to DFT theory, the diazotization and coupling reaction between p-aminobenzenesulfonic acid and nitrite ion under acidic conditions are theoretically calculated, the reaction mechanism is explored, the configuration of the final product is determined, and the UV-vis Spectrum of the product is calculated to provide a theoretical basis for the detection of nitrogen dioxide, It can also provide a reference for the improvement of experiments and the development of nitrogen dioxide detection technology in the future.

## 2. Experimental Method

All calculations were performed using Gaussian 09[7] package. Using the method of density functional theory [8], at the level of B3LYP/6-311$^{++}$G (D,P) [9], the structures of all reactants, intermediates, transition states and products are optimized respectively. Through the vibration analysis of the optimized structure, it is confirmed that there is no virtual frequency at each equilibrium point, and it is concluded that the minimum point on the potential energy surface is the optimized structure, and all transition states have and only one virtual frequency, The intrinsic reaction coordinate[10] (IRC) calculation method is used to track the transition state, calculate the energy of reactants, intermediates, transition states and products on the reaction path at the same level, and obtain their corresponding single point energy and zero correction energy. Finally, the UV-vis Spectrum of the product is calculated by TDDFT method.

## 3. Results and Discussions

### *3.1. Reaction Path Analysis*

Under acidic conditions, nitrite ions are first converted into electrophilic $NO^+$, and electrophilic $NO^+$ attacks amino N to produce nitrosamines. The generated nitrosamines are rearranged, the hydroxyl groups in the molecules are combined with hydrogen protons to form water, and then removed to produce diazonium salts; Diazonium salt acts as an electrophilic reagent to attack amino para or ortho C to produce an intermediate product, which releases protons to produce azo compounds. The reaction path includes two elementary reactions, the first is the diazotization reaction of aryl primary amine and nitrous acid, and the second is the coupling reaction of diazonium salt and 1-naphthylamine. Because the para position and ortho position of 1-naphthylamine can react, two reaction paths path1 and path2 are proposed, in which path1 contains three elementary reactions, namely Step1, Step2 and Step3; Path2 contains three elementary reactions, Step1, Step2 and Step4, that is, diazonium salt and 1-naphthylamine undergo electrophilic substitution reactions at ortho and para positions to produce corresponding azo compounds. The reaction path is shown in Figure 1.

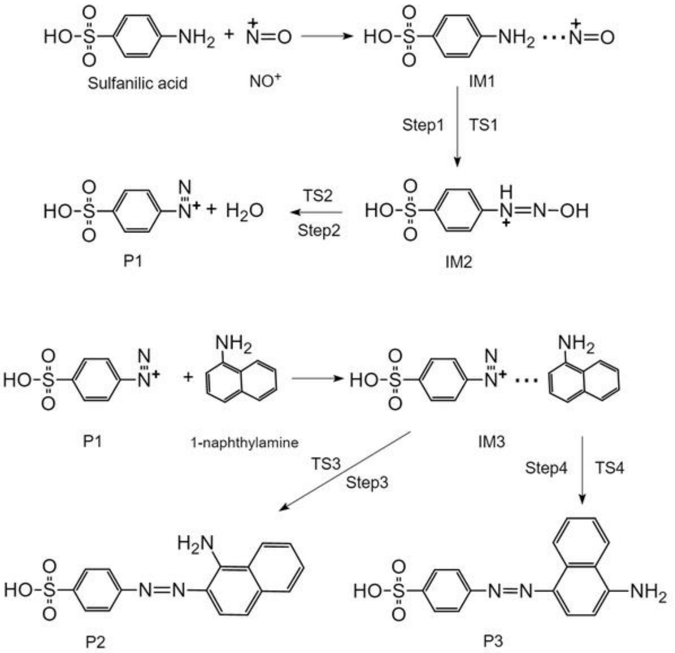

*Figure 1: Reaction path*

After structural optimization and vibration analysis of the optimized structure of reactants, intermediates, transition states and products, the main bond length information of reactants, intermediates, transition states and products is shown in Table 1.

*Table 1: Main key length information*

| Compound | N(15)-N(19) | C(2)-N(15) | N(15)-H(16) | N(19)-O(20) |
|---|---|---|---|---|
| Sulfanilic acid | | 0.13817 nm | 0.10078 nm | |
| IM1 | | 0.13981 nm | 0.10169 nm | |
| TS1 | 0.14811 nm | 0.14483 nm | 0.14552 nm | 0.12197 nm |
| IM2 | 0.12565 nm | 0.14153 nm | 0.10300 nm | 0.13258 nm |
| TS2 | 0.12439 nm | 0.13901 nm | 0.13626 nm | 0.14836 nm |
| P1 | 0.11044 nm | 0.13853 nm | | |

Taking path1 as an example, p-aminobenzenesulfonic acid forms IM1 close to $NO^+$, the distance between N (15)-H (17) is 0.10169 nm, and the distance between N (15)-N (19) is 0.21524 nm. Because N (19) carries a positive charge and approaches N (15) as an electrophilic reagent, O (20) attracts H (17) and forms TS1. At this time, the distance between N(15)-N(19) is shortened to 0.14811 nm, and

N(15)-N(19) forms a single bond, The distance between H(17)-O(20) is 0.12230 nm, and the distance between N(15) and H(17) is extended to 0.14552 nm; Then the distance of N(15)-N(19) continued to shorten to 0.12565 nm, N(15)-N(19) formed a double bond, H(17)-O(20) shortened to 0.09739 nm, H(17)-O(20) formed a single bond, and IM2 was formed since then; Then, the distance between N(15)-H(16) and N(19)-O(20) lengthens, and H(16) approachesO(20) to form TS2. At this time, the distance between N (15)-H (16) is 0.13626 nm, the distance between N (19)-O (20) is 0.14836 nm, and the distance between H (16) and O (20) is 0.12400 nm; Then, the distance between H (16) and O (20) continued to shorten to 0.09649 nm. H (16)-O (20) formed a single bond, formed a molecule of water, eliminated and obtained diazonium salt. Since then, Step 1 was completed. Then 1-naphthylamine was added, and the two molecules were close to each other to form IM3. At this time, the distance between C (14) and N (37) was 0.28620 nm; Then, the distance between N (35)-N (37) and the distance between C (14) and N (37) is shortened to form TS3. At this time, the distance between N (35)-N (37) is 0.12566 nm, N (35)-N (37) forms a double bond, the distance between C (14) and N(37) is 0.14660 nm, C(14)-N(37) forms a single bond, and then H(17) disappears to form an ortho substitution product P2.

### *3.2. IRC Path Analysis*

In order to determine the authenticity of the connection between the transition state and the configuration of reactants, intermediates and products in the reaction, IRC path analysis was carried out for the four transition states TS1, TS2, TS3 and TS4. The change of their respective reaction potential energy with the reaction coordinate s is shown in Figure 2, in which the highest points of the curve are each transition state. The calculation results show that the molecular configurations displayed at both ends of the IRC curve point to their corresponding reactants and products respectively, and the four transition states can be obtained, which are the real transition states on the reaction path.

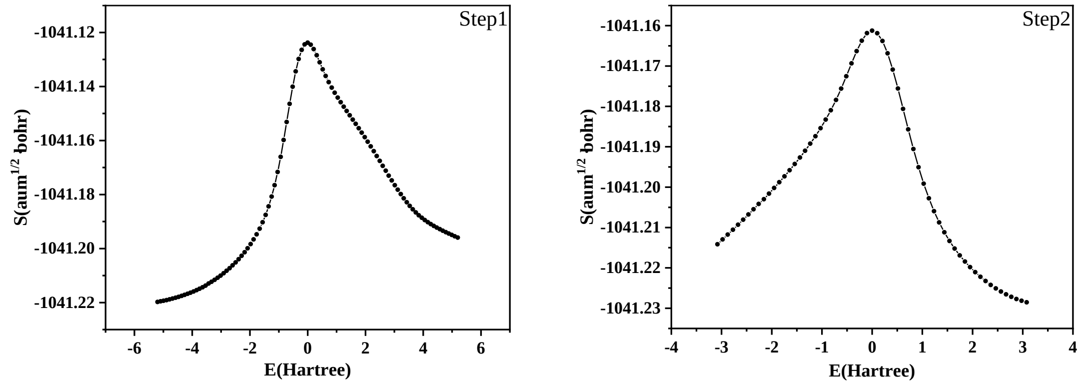

(a)Step1 (b)Step2

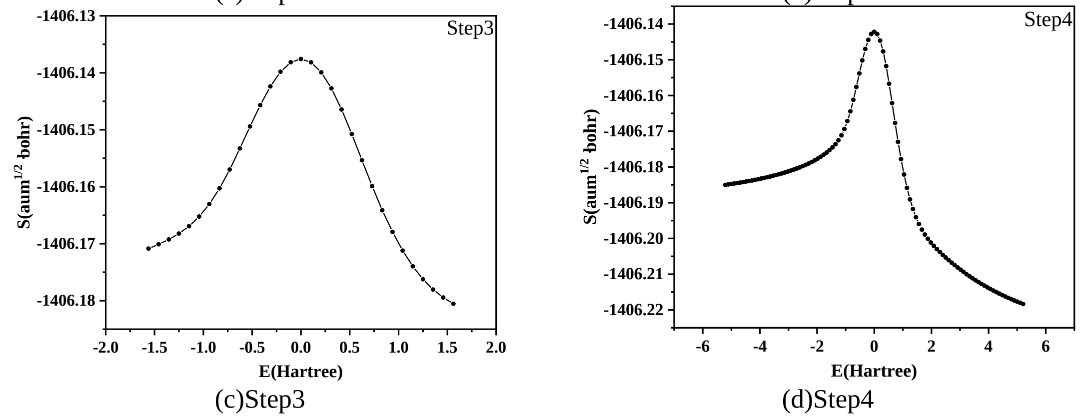

(c)Step3 (d)Step4

*Figure 2: Reaction path*

### *3.3. Reaction Energy Analysis*

In order to calculate the activation energy of each elementary reaction, the single point energy G, the corresponding zero correction energy ZPE and the relative energy of each substance in the elementary reaction were calculated by density functional theory *ΔE*. As shown in Table 2, the potential energy profile of each elementary reaction step is shown in Figure 3.

*Table 2: Energy and relative energy of reactants, intermediates, transition states and products*

| Compound | *G*/(a. u. ) | ZPE/(a. u. ) | *ΔE*/ kJ $mol^{-1}$ |
|---|---|---|---|
| R1 | 1041.0856 | 0.137051 | 0 |
| IM1 | 1041.1320 | 0.138593 | -121.9 |
| TS1 | 1041.0313 | 0.133808 | 142.5 |
| IM2 | 1041.1305 | 0.140632 | -118.1 |
| TS2 | 1041.0673 | 0.134024 | 48.0 |
| P1 | 1041.0860 | 0.137808 | -1.1 |
| R2 | -1045.9290 | 0.274311 | 0.0 |
| IM3 | -1405.9690 | 0.275969 | -105.0 |
| TS3 | -1405.9173 | 0.273505 | 30.8 |
| P2 | -1405.9331 | 0.274048 | -10.7 |
| R3 | -1405.9304 | 0.273999 | 0.0 |
| IM4 | -1405.9679 | 0.276437 | -98.2 |
| TS4 | -1405.9197 | 0.273624 | 28.2 |
| P3 | -1405.9329 | 0.273755 | -6.3 |

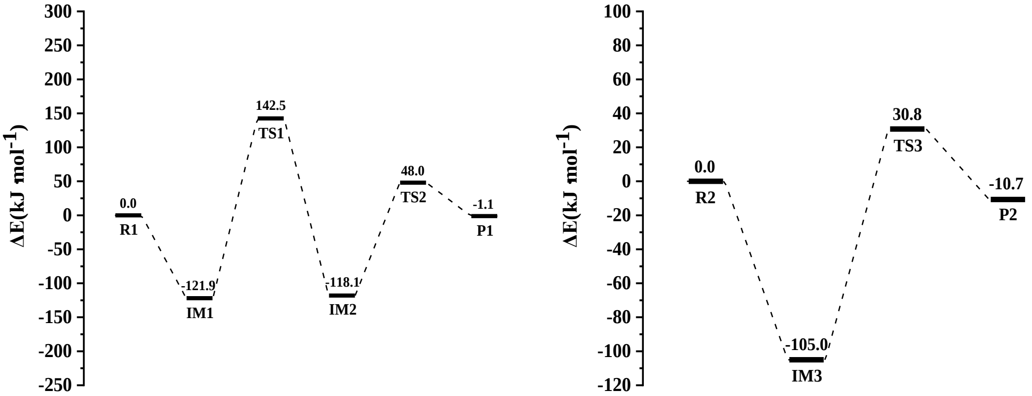

(a)Step1+Step2 (b)Step3

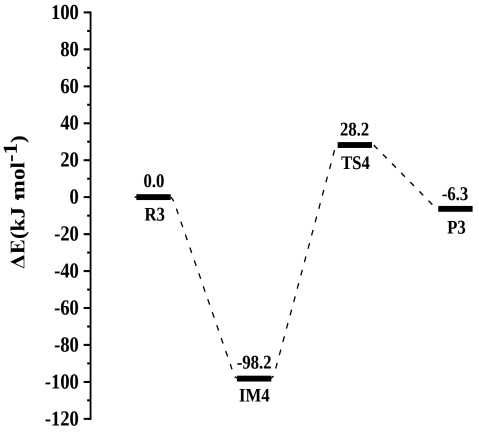

(c)Step4

*Figure 3: Potential energy profile of each reaction step*

According to the calculation, the activation energies of Step1~Step4 are 264.4 kJ $mol^{-1}$, 166.1 kJ $mol^{-1}$, 135.8 kJ $mol^{-1}$ and 126.4 kJ $mol^{-1}$ respectively. Step1 is an electrophilic substitution reaction, and the activation energy is the largest, which is mainly due to the generation of TS1 when the affinity proton $NO^+$ is close to the reactant, accompanied by the breaking and formation of chemical bond, as well as the rotation of bond angle. Step2 is the elimination reaction to remove a molecule of water, The activation energy is also relatively large, because when O(20) attracts H(16) in the process of removing water molecules, it will increase the bond length of N(15)─H(16) and rotate at a certain angle. Therefore, it has large activation energy. Both Step3 and Step4 are electrophilic substitution reactions. Because the structures of TS3 and TS4 are larger than those of TS1 and TS2, the stability of TS3 and TS4 is lower, the activation energy of electrophilic substitution reaction is also relatively small. In the whole reaction process, electrophilic substitution reaction Step1 is a speed control step.

### *3.4. UV-vis Spectrum Calculation*

TDDFT calculations were performed on the reactant p-aminobenzene sulfonic acid and the ortho product P2 and para product P3 generated by Step2 and Step4, respectively, to obtain their UV-vis spectra. The results are shown in Figure 4. It can be seen that the reactant p-aminobenzene sulfonic acid has no obvious absorption in the visible region, and the ortho product P2 and para product P3 have obvious absorption peaks in 400 nm~500 nm. In terms of peak intensity, the ortho product P2 is higher than the para product P3, which also proves that the products obtained from the reaction of p-aminobenzene sulfonic acid and 1-naphthylamine as chromogenic agents in Chapter2 have obvious absorption in the visible region. Therefore, it shows that ortho and para azo compounds are indeed generated after diazotization and coupling reaction.

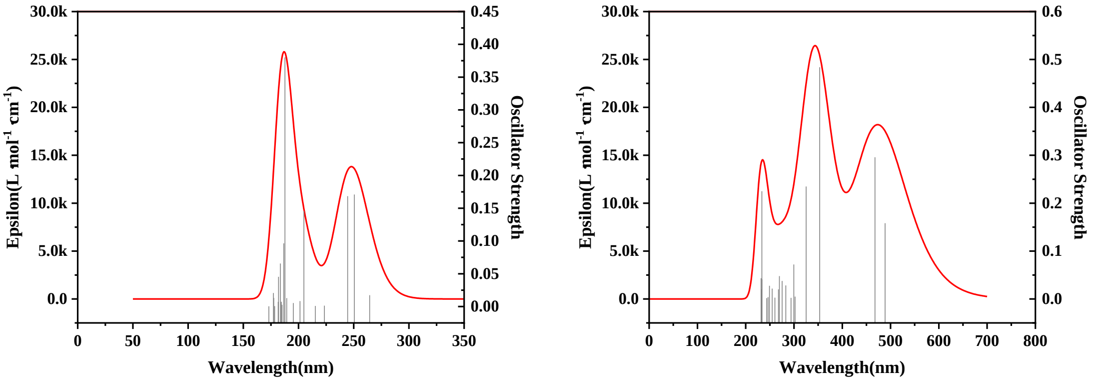

(a)Sulfanilic acid (b)P2

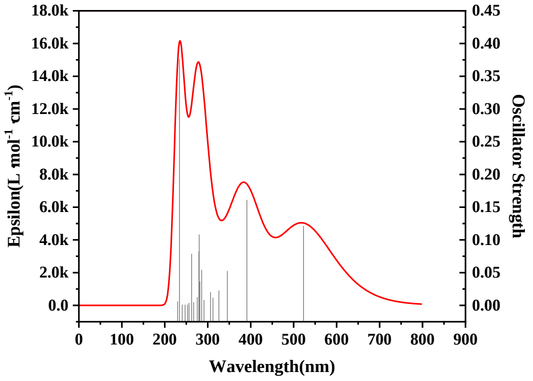

(c)P3

*Figure 4: UV-vis spectra of reactants and products P2 and P3*

## 4. Conclusion

Through the method of quantum mechanics and density functional theory, the mechanism of diazonization and coupling reaction of nitrite ions to form diazonium salt under acidic conditions is studied, and the following conclusions are obtained:

(1) There are two intermediates and two transition states in the process of diazonization reaction to produce diazonium salt. Step1 is the rate control step of the whole reaction and the activation energy is 264.4 kJ $mol^{-1}$

(2) In the process of diazonium salt coupling reaction, ortho and para products appeared. It was verified that they really existed, and the activation energies were 135.8 kJ $mol^{-1}$ and 126.4 kJ $mol^{-1}$

(3) The UV-vis spectra of products P2 and P3 were obtained by TDDFT calculation. The results show that products P2 and P3 have absorption in the visible region, which is consistent with the actual experimental results.

## References

*[1] Liu J, Li S, Zhang B, et al. Ultrasensitive and low detection limit of nitrogen dioxide gas sensor*

*based on flower-like ZnO hierarchical nanostructure modified by reduced graphene oxide [J]. Sensors and Actuators B: Chemical, 2017, 249: 715-724.*

*[2] St. John J C, Chameides W L, Saylor R. Role of anthropogenic NOx and VOC as ozone precursors: A case study from the SOS Nashville/Middle Tennessee Ozone Study[J]. Journal of Geophysical Research: Atmospheres, 1998, 103(D17): 22415-22423.*

*[3] Peng H, Li F, Hua Z, et al. Highly sensitive and selective room-temperature nitrogen dioxide sensors based on porous grapheme [J]. Sensors and Actuators B: Chemical, 2018, 275: 78-85.*

*[4] Zhang C, Wang J, Geng X. Tungsten oxide coatings deposited by plasma spray using powder and solution precursor for detection of nitrogen dioxide gas[J]. Journal of Alloys and Compounds, 2016, 668: 128-136.*

*[5] Wang X D.Study of the damage effect of nitrogen dioxide and its derivatives on lung and brain [D]. Shanxi University, 2014.*

*[6] Li H Y.*$NO_2$ *inhalation contributes to the development and progression of ischemic stroke and vascular denmentia in rat [D]. Shanxi University, 2013.*

*[7] J F M, W T G, B S H. Gaussian 09, Gaussian, Inc. [J]. Wallingford CT, 2009.*

*[8] Parr R G. Density Functional Theory of Atoms and Molecules [J]. 1980, 76(6): 2522-2526.*

*[9] Jacquemin D, Perpete E A, Ciofini I, et al. On the Performances of the M06 Family of Density Functionals for Electronic Excitation Energies [J]. Journal of Chemical Theory & Computation, 2010, 6(7): 2071-2085.*

*[10] Gonzalez C, Schlegel H B. An improved algorithm for reaction path following [J]. Journal of Chemical Physics, 1989, 90(90): 2154-2161.*